Pertanika J. Sci. & Technol. 33 (3): 1563 - 1593 (2025)

PERTANIKA JOURNALS

SCIENCE & TECHNOLOGY

Journal homepage: http://www.pertanika.upm.edu.my/

Investigation of Aged-related Metabolites in the Marine Polychaete (*Marphysa moribidii*) Using ^{1}H NMR Metabolomics and LC-MS/MS Analysis

Nurfarah Aini Mocktar[1], Mohamad Sofi Abu Hassan[2], Maulidiani Maulidiani[1], Wan Iryani Wan Ismail[1,3], Izwandy Idris[4,5], Farhanini Yusoff[1] and Noor Aniza Harun[1,2,6]*

[1]Faculty of Science and Marine Environment, Universiti Malaysia Terengganu, Kuala Nerus, 21030 Terengganu, Malaysia

[2]Higher Institution Centre of Excellence (HICoE), Institute of Tropical Aquaculture and Fisheries, Universiti Malaysia Terengganu, Kuala Nerus, 21030 Terengganu, Malaysia

[3]Cell Signalling and Biotechnology Research Group (CeSBTech), Faculty of Science and Marine Environment, Universiti Malaysia Terengganu, Kuala Nerus, 21030 Terengganu, Malaysia

[4]South China Sea Repository and Reference Centre, Institute of Oceanography and Environment, Universiti Malaysia Terengganu, Kuala Nerus, 21030 Terengganu, Malaysia

[5]Mangrove Research Unit (MARU), Institute of Oceanography and Environment, Universiti Malaysia Terengganu, Kuala Nerus, 21030 Terengganu, Malaysia

[6]Advanced Nano Materials (ANOMA) Research Interest Group, Faculty of Science and Marine Environment, Universiti Malaysia Terengganu, Kuala Nerus, 21030 Terengganu, Malaysia

ABSTRACT

Marphysa moribidii (marine polychaetes) exhibits distinct age-related characteristics based on body width in the initial seven chaetigers, excluding parapodia or bristles that are classified into three age classes: Class I (body width ranging from 3–5 mm), Class II (6–8 mm), and Class III (9–11 mm). Despite its potential, the exploration of metabolites in marine worms, particularly through metabolomics, remains limited. The aim of this study is to identify the metabolite profile and depict the metabolic pathways of different age classes of *M. moribidii* utilising proton nuclear magnetic resonance spectroscopy (^{1}H NMR) metabolomics and liquid chromatography with tandem mass spectrometry (LC-MS/MS) analysis. A total of 35 metabolites were identified using ^{1}H NMR metabolomics, including amino acids, carbohydrates, fatty acids, glycerol, nitrogenous compounds, organic compounds, and vitamins. LC-MS/MS analysis also discovered 36 metabolites that can be categorised into organic acids, carbohydrates, phenolic compounds, fatty acids, and amino acids. Class II *M. moribidii* emerged to have

ARTICLE INFO

Article history:
Received: 23 September 2024
Accepted: 31 January 2025
Published: 23 April 2025

DOI: https://doi.org/10.47836/pjst.33.3.21

E-mail addresses:
farahaini145@yahoo.com (Nurfarah Aini Mocktar)
sofie1495@gmail.com (Mohamad Sofi Abu Hassan)
maulidiani@umt.edu.my (Maulidiani Maulidiani)
waniryani@umt.edu.my (Wan Iryani Wan Ismail)
izwandy.idris@umt.edu.my (Izwandy Idris)
farhanini@umt.edu.my (Farhanini Yusoff)
nooraniza@umt.edu.my (Noor Aniza Harun)
* Corresponding author

e-ISSN: 2231-8526

the highest concentration of chemicals originating from amino and fatty acids, making it the ideal age for harvesting. Comparing the metabolite profiles across different age groups of *M. moribidii* could provide valuable insights into its physiological processes, metabolic dynamics, and potential bioactive compounds present at various developmental stages.

Keywords: ^{1}H NMR metabolomics, LC-MS/MS analysis, *Marphysa moribidii*, metabolite profiles, polychaete

INTRODUCTION

Polychaetes are a class of marine worms belonging to the phylum Annelida, which includes over 12,000 known species, such as bloodworms, ragworms, and sea mice (Capa & Hutchings, 2021). Polychaetes are segmented worms characterised by the presence of parapodia, which are paired fleshy protrusions covered in numerous bristles known as chaetae. These leg-like parapodia, adorned with an array of bristles, serve as polychaetes' most prominent and distinguishing features (Glasby & Timm, 2008; Verdonschot, 2015). *Marphysa* is one of the nine genera in the family *Eunicidae*. It comprises around 60 species, which are variously classified based on several characteristics such as the type of subacicular chaetae, shape of the prostomium, location of branchiae initiation, or shape of the pectinate chaetae (Zanol et al., 2016).

Marphysa moribidii is the marine baitworm of the genus *Marphysa* in the family *Eunicidae* that can be found in the mangrove forest on the west coast of Peninsular Malaysia. It is a main baitworm species collected by bait diggers and mostly found in large numbers around the stilt roots of *Rhizophora apiculata* (Idris & Arshad, 2013; Idris & Hutchings, 2014). *M. moribidii* is classified into three age classes depending on their body width. Through this evaluation, the polychaetes can be divided into three different classes: Class I (body width ranging from 3–5 mm), Class II (body width ranging from 6 – 8 mm), and Class III (body width ranging from 9–11 mm) (Rosman et al., 2021).

Research on *M. moribidii* has been performed, and this species has not been utilised as a baitworm. Recent studies have explored the potential of *M. moribidii* in acute wound healing, demonstrating its unique ability to regenerate damaged posterior segments (Rapi et al., 2020). Furthermore, chemical compounds such as alkaloids, phenolics, amino acids, and organic acids have been identified in *M. moribidii* extracts, suggesting their potential contribution to the wound-healing process (Rapi et al., 2020). Additionally, the utilisation of crude extract of *M. moribidii* as a biogenic reducing agent has resulted in significant advancements in the eco-friendly production of silver nanoparticles (Rosman et al., 2020) and gold nanoparticles (Pei et al., 2020; Hassan et al., 2023).

Metabolomic is a broad approach that facilitates identifying and quantifying both endogenous and exogenous metabolites in biological organisms influenced by genetic and environmental factors (Patel et al., 2021). Nevertheless, metabolomics is still not widely

applied in the research of marine worm metabolites despite its enormous potential. To the best of our knowledge, *M. moribidii's* metabolomic pathways have not yet been reported. The analytical methods that can be utilised to ascertain the structures of a wide variety of metabolite classes are ^{1}H NMR and LC-MS/MS techniques. Both analytical tools have been extensively used in metabolomics research (Marion, 2013; Emwas et al., 2019; Gathungu et al., 2020; Moco, 2022).

During the wet season, low salinity affects the allelochemicals of *M. moribidii*, influencing its metabolites, including amino acids, organic acids, fatty acids, sterols, and aromatic compounds. *M. moribidii* exhibits stress responses and higher mortality under low salinity. Seasonal variations significantly impact its metabolite profile, as indicated by different FTIR profiles (Wijaya et al., 2024).

Marine polychaetes have shown potential in medical applications, such as antioxidant and wound-healing properties. A positive correlation exists between DPPH activity and total phenolic content (TPC), suggesting that TPC contributes to antioxidant activity. FTIR spectra revealed characteristic signals of polysaccharides, lipids, and carbohydrates. The ATR-FTIR metabolomics approach effectively analysed the chemical profile of polychaete, revealing limited antioxidant activity (Zamzam et al., 2021).

This study extensively explored the metabolite profiles of marine invertebrates *M. moribidii* using the ^{1}H NMR metabolomics approach and LC-MS/MS analysis. This study aims to identify the metabolite profile and depict the metabolic pathways of *M. moribidii* development at various age classes. Given the success of *M. moribidii* in various applications, including the production of noble metallic nanoparticles and wound treatment, it becomes crucial to investigate the chemical compositions of this marine worm to gain a deeper understanding of its biochemical pathways. The chemical constituents of *M. moribidii* can be explored to identify substances that may have potential applications in agriculture, materials science, food, and other areas. A knowledge of these molecular constituents will yield discernment about the worm's physiology, ecological role, and behaviour, in addition to its metabolic processes and the mechanism that supports its growth, maturation, and ageing.

MATERIALS AND METHODS

Chemicals

LC-MS/MS grade methanol, acetonitrile, formic acid (Merck, Darmstadt, Germany), and de-ionised water were used as the mobile phase in LC-MS/MS analysis. For ^{1}H NMR analysis, deuterium oxide (D_2O) containing 0.1% 3-(trimethylsilyl) propionic-2,2,3,3-d_4 acid sodium salt (TSP) was employed to selectively obtain signals from the hydrogen atoms in the sample.

M. moribidii Sampling

Individuals of *M. moribidii* were collected from a mangrove strip in Morib, Selangor, within the *Rhizophora apiculata* zonation (2.75827ºN 101.4379ºE) with the sampling surveys took place in April 2021 when low tide occurred. After gently removing the polychaetes from the mangrove roots, they were transferred into a container containing natural sediment before transportation to the laboratory. To ensure acclimatisation, *M. moribidii* was then placed in an artificial aquarium that mimicked their natural habitat (salinity 30) before proceeding with the experiment.

Identification of M. *moribidii* and Size (Body Width) Classification

Marphysa moribidii classes were assessed and classified according to their body width as recommended by (Occhioni et al., 2009), where it can be divided into three categories: Class I (3–5 mm), Class II (6–8 mm), and Class III (9–11 mm), with measurements taken from the first seven chaetigers of each polychaete (Górska et al., 2019). Notably, these measurements excluded parapodia or bristles.

Preparation of *M. moribidii* Extract

Fresh specimens of *M. moribidii* weighing 15 g from different age classes, namely Class I (body width: 3–5 mm), Class II (body width: 6–8 mm) and Class III (body width: 9–11 mm) were cleaned using artificial seawater and ddH_20 to remove any sediments and dried using tissue paper. The polychaete was dissected and pulverised using a mortar and pestle. The resulting crude extract was mixed with 100 mL of ddH_2O and allowed to incubate at room temperature for 1 hour to facilitate the extraction of bioactive compounds. It was then filtered using the Whatman No.1 filter paper (Rosman et al., 2021). The resulting filtrates were stored at -80°C before undergoing freeze-drying to remove excess water from the polychaete bodies. The dried crude extract obtained from *M. moribidii* was subsequently used for further analysis.

Identification of *M. moribidii* and Size (Body Width) Classification Using Stereo Zoom Microscope

Polychaetes of different age classes were preserved in 70% ethanol for morphological examinations. The specimens were positioned on the stage plate directly beneath the objective lens for viewing. A stereo microscope (Olympus SZ) was utilised, employing natural light that reflected from the specimen for observation.

Sample Preparation for ^{1}H NMR

About 100 mg of the freeze-dried crude extract from the polychaete samples was placed in a microcentrifuge tube. The sample was then resuspended in 700 µL of 99.9% D_2O

containing 0.1% TSP and sonicated for 30 minutes at room temperature. All samples were vortexed for 10 min at 1300 rpm to ensure a homogeneous mixture. Subsequently, 600 µL of the supernatant solution was transferred to an NMR tube for ^{1}H NMR analysis.

^{1}H NMR Spectroscopy Analysis

The ^{1}H NMR measurements were performed using a Varian INOVA NMR spectrometer (Varian Inc., CA, USA) operating at a frequency of 499.89 MHz and maintained at 25°C. The NMR analysis was conducted for each of the three different age classes with four replicates per class. Each sample was acquired with 64 scans, an acquisition time of 220 s, a pulse width of 3.75 ms, and a relaxation delay of 2.0 s. The spectral width was adjusted to cover the 1.00 and 20.00 ppm range. All spectra were manually phased and baseline corrected.

Data Processing and Multivariate Data Analysis

The Chenomx Processor software (Version 5.1, Alberta, Canada) was utilised to preprocess ^{1}H NMR spectra, ensuring a consistent configuration across all sample spectra. Each spectrum was manually processed with phasing and baseline corrections, and TSP was selected as the reference peak at δ 0.00. Water-containing regions between δH 4.57 and 4.95 were excluded from all spectra. All ^{1}H NMR spectra were binned (bin size of 0.04) using Chenomx Profiler software (Version 5.1, Alberta, Canada) to obtain 243 data points, which will be subjected to multivariate data analysis (MVDA) as the x-variables input data. MVDA models such as principal component analysis (PCA) and orthogonal partial least square discriminant analysis (OPLS-DA) were conducted using SIMCA-P 14.1 (Umetrics AB, Umeå, Sweden). Prior to analysis, the data were Pareto scaled to minimise variance distortion. The dataset was initially subjected to PCA to visualise and differentiate groups based on their metabolites, providing an overall overview of the dataset. The NMR spectral data were subjected to OPLS-DA models to further distinguish between classes. The OPLS-DA model was applied to discriminate between two groups (classes) of the polychaetes of different ages. Probable metabolites contributing to the different age classes were identified based on the loading column plot. The OPLS-DA model was validated using CV-ANOVA, with a p-value < 0.05 indicating the model's statistical significance. The supervised model was also validated using permutation tests, with 20 permutations carried out in this study.

Identification of Metabolites Based on ^{1}H NMR Analysis

The diversity of metabolites associated with these different ages of *M. moribidii* was identified by comparing their chemical shifts in ^{1}H NMR spectra with the chemical shifts of standard compounds available in the Human Metabolome Database Data Bank (HMDB)

(http://www.hmdb.ca/metabolites) and literature. The identification of metabolites was performed using Chenomx Profiler software (Version 5.1, Alberta, Canada). The metabolic pathways were determined using MetaboAnalyst software (http://www.metaboanalyst.ca/). MetaboAnalyst is a web-based platform offering a suite of metabolomics data analysis tools, including pathway analysis, PCA and OPLS-DA. It provides a user-friendly interface and integrates various statistical and bioinformatics methods for data preprocessing, normalisation, and visualisation.

LC-MS/MS Data Analysis and Metabolite Identification

The LC-MS/MS analysis was carried out on a Vion IMS LC-QTOF-MS (Waters, USA). The liquid chromatography was separated using an ACQUITY UPLC BEH C18 column (2.1 X 50 mm, 1.7 µm) with a gradient solvent system of 0.1% formic acid in water and 0.1% formic acid in acetonitrile. The injection volume was 10 µL, and the flow rate was maintained at 0.4 mL/min for 35 min. The mass spectra were acquired in ESI negative ion mode with the parameters: Capillary voltage 2.50 kV, source temperature 120°C, desolvation temperature 550°C, desolvation gas 800 L/h, and cone gas 50 L/h. The acquired spectra were analysed using the in-house software UNIFI (Version 1.8; Waters Corporation). Metabolite identification was conducted by comparing the retention time and MS/MS data of the sample with the reference compound available in the library. Additionally, the identification of metabolites was verified by comparing them with the literature and consulting available online databases (http://www. metabolomicsworkbench.org).

Statistical Analysis

Relative quantification of identified metabolites was performed using the signals of metabolites of interest obtained from the binning dataset. Statistical analysis, including One-way ANOVA and Tukey's honest significant difference (Tukey-HSD) multiple-comparison, was conducted using MetaboAnalyst software (http://www.metaboanalyst.ca/). The p-values of <0.05 were considered statistically significant. Supplementary Table 1 in APPENDIX shows the One-way ANOVA and Tukey-HSD Pairwise Test results of the identified metabolites in M1, M2, and M3, along with boxplots comparing the different classes of polychaete samples.

RESULTS AND DISCUSSION

Identification of M. *moribidii* and Size (Body Width) Classification

Body width is commonly used as a standard method to determine the age class of polychaetes, as recommended by Occhioni et al. (2009). The findings indicate that body size variations among populations are stronger than shape. The identification of *M.*

moribidii samples in this study did not involve molecular techniques but relied on morphological comparisons. The detailed morphological features likely focused on external and internal anatomical characteristics, which serve as distinguishing traits among species within the genus *Marphysa* identified by Idris and Hutchings (2014). *M. moribidii* is classified into three age groups based on body width: young (M1) with a body width of 3–5 mm, adult (M2) with 6–8 mm, and old (M3) with 9–11 mm. This classification allows for studying how the metabolite profiles of *M. moribidii* evolve with age, aiding in the identification of metabolic variations. These metabolic changes may reflect physiological, biochemical, or ecological adaptations, providing insights into how the species interacts with its environment (Glasby et al., 2021). The images of *M. moribidii* representing different age classes based on their body width are presented in Figure 1. To facilitate clarity throughout the discussion, the notations M1, M2 and M3 have been assigned to represent each respective class of *M. moribidii* (Table 1).

Table 1
Different age classes of M. moribidii *based on their body width (mm)*

Class	Sample Notation	Width (mm)
I	M1	3 – 5
II	M2	6 – 8
III	M3	9 – 11

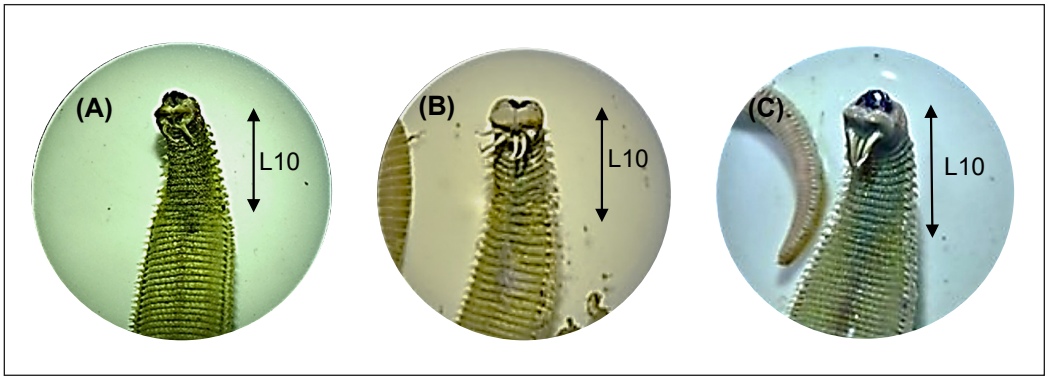

Figure 1. M. moribidii images under stereo zoom microscope of (A) Class I (3–5 mm), (B) Class II (6–8mm), and (C) Class III (9–11mm) (Olympus SZ); Scale bar: 100 µm

Metabolite Variations of Different Ages of *M. moribidii* Determined by ^{1}H NMR Metabolomics

Chemical constituents presented in the polychaete extract were identified using ^{1}H NMR analysis, a robust technique for compound identification in complex mixtures. The ^{1}H NMR spectra of the *M. moribidii* extract (Supplementary Figure 1) revealed the presence of various compounds (35 metabolites), including amino acids, organic compounds, nitrogenous compounds, vitamins, carbohydrates, and fatty acids (Table 2). Based on the

^{1}H NMR signals, the amino acids of phenylalanine, betaine, isoleucine, leucine, glycine, alanine, glutamic acid, methionine, L-aspartic acid, beta-alanine, valine and taurine were discovered. Phenylalanine was identified based on the signals observed at δH 7.41 (m), 7.36 (m), and 7.31 (m). Tentatively, singlets at δH 3.89 and 3.25 were assigned as betaine, and δH 3.55 was assigned to glycine. The characteristic signals for taurine were observed at δH 3.42 (t) and 3.25 (t). Meanwhile, multiple signals for methionine were also identified at δH 3.85 (m), 2.63 (m), 2.19 (m) and a singlet at δH 2.13.

The ^{1}H NMR spectra exhibited singlets signals for organic compounds at δH 3.65, 2.22, 2.27, 1.91, 3.12, 2.39 and 8.45, corresponding to glycerol, acetone, acetoacetic acid, acetate, malonic acid, succinic acid and formic acid, respectively. Some nitrogenous compounds identified were creatinine, observed at δH 4.05 (s) and 3.04 (s), and creatine at δH 3.92(s) and 3.03(s) along with trimethylamine at δH 2.88 (s). Furthermore, the ^{1}H NMR spectra revealed characteristic signals of fatty acids, including peaks at δH 5.34 (t), 1.22 (m), and 0.89 (t). Various signals corresponding to carbohydrates, such as sucrose and glucose, were also observed. Two metabolites from the vitamin group were also presented, exhibiting signals at δH 9.11(s), 8.82(m), 8.83(m), 8.07(m), 4.43(s) for trigonelline, and a singlet at δH 4.06, 3.51, and 3.19 for choline.

The experiments involved three distinct age classes of *M. moribidii, which* were subjected to ^{1}H NMR metabolomics to evaluate their metabolite variations. MVDA via PCA model was employed to reveal underlying patterns within the data in a two-dimensional representation (Figure 2A). The PCA model resulted in five principal components, with PC1 and PC2, considered the most informative for visualising and interpreting the data. The total variation explained by the PC1 and PC2 was 93.6%, which is sufficiently high to effectively describe the dataset. The R^2X cumulative value of 0.991 and Q^2 cumulative value of 0.961 further confirm that the PCA model is reliable and excellent. By examining the PCA loadings plot (Figure 2B), it was possible to identify metabolites associated with the observed clustering. These PCA-selected metabolic features were further validated and supplemented using OPLS-DA modelling. This binary classification approach facilitates discrimination analysis to extract metabolic markers that differentiate sample groups as depicted by the PCA models.

Table 2
Summary of the ^{1}H NMR metabolites assignment of M. moribidii*, which categorises the different groups of metabolites and their respective signals*

Group	Metabolite	Chemical shift (ppm)
Amino acid	Phenylalanine	7.41 (m), 7.36 (m), 7.31 (m), 4.00 (s, overlap), 3.28 (m, overlap), 3.11 (m, overlap)
	Betaine	3.89 (s), 3.25 (s)
	Isoleucine	1.00 (d), 0.93 (t)

Table 2 *(continue)*

Group	Metabolite	Chemical shift (ppm)
	Leucine	0.95 (t), 0.94 (t)
	Glycine	3.55 (s)
	Alanine	1.47 (d)
	Glutamic acid	3.75 (s), 2.36 (m), 2.33 (m), 2.12 (m), 2.04 (m)
	Methionine	3.85 (m), 2.63 (m), 2.19 (m), 2.13 (s), 2.11 (m)
	L-Aspartic acid	2.80 (m), 2.67 (m)
	β-Alanine	3.17 (m), 2.54 (t)
	Valine	1.03 (d), 0.98 (d)
	Taurine	3.42 (t), 3.25 (t, overlap)
Organic compound	Acetone	2.22 (s)
	Acetoacetic acid	2.27 (s)
	Acetamide	7.54 (s), 6.78 (s), 1.99 (s)
	Sn-Glycero-3-phosphocholine (GPC)	4.31 (s), 3.94 (m, overlap), 3.91 (m, overlap), 3.87 (m, overlap), 3.67 (m), 3.22 (s)
	Glycerol	3.78 (s), 3.65 (m), 3.55 (m)
	Short-chain keto acids (SCKA)	1.60–1.80 (m), 1.35–1.45 (m), 0.80–0.90 (t)
	Acetate	1.91(s)
	Lactic acid	4.11 (m), 1.34 (d)
	Malonic acid	3.12 (s)
	Succinic acid	2.39 (s)
	2-Oxoglutaric acid	3.00 (t), 2.43 (t)
	Formic acid	8.45 (s)
	Inosinic acid (IMP)	8.56 (s), 8.22 (s, overlap), 6.13 (d, overlap), 4.50 (m, overlap), 4.36 (m, overlap), 4.03 (m, overlap), 4.00 (m, overlap)
	Inosine	8.33 (s), 8.22 (s), 6.08 (m), 4.77 (s), 4.43 (s), 4.27 (s), 3.91 (m, overlap), 3.83 (m, overlap)
	4-Hydroxyphenylacetic acid (4-HPA)	7.15 (m), 6.85 (m), 3.42 (s)
Nitrogenous compound	Creatinine	4.05 (s), 3.04 (s)
	Creatine	3.92 (s), 3.03 (s)
	Trimethylamine (TMA)	2.88 (s)
Carbohydrate	Sucrose	5.40 (d), 4.21 (d), 4.04 (t), 3.88 (overlap), 3.82 (m), 3.80 (m),3.76 (m), 3.69 (s), 3.55 (overlap), 3.47 (t)
	Glucose	5.23 (d), 4.64 (d), 3.89(m), 3.84 (m), 3.76 (m), 3.53 (m), 3.48 (m), 3.39 (m), 3.23 (t, overlap)
Vitamin	Trigonelline	9.11 (s), 8.82 (m), 8.83 (m), 8.07 (m), 4.43 (s)
	Choline	4.06 (s), 3.51 (s), 3.19 (s)
Fatty acid		5.34 (t), 1.22 (m), 0.89 (t, overlap)

s = singlet, d = doublet, t = triplet, and m = multiplet

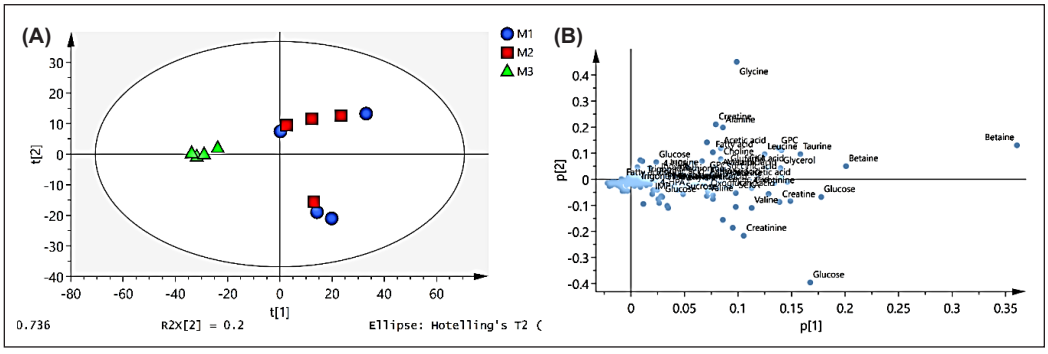

Figure 2. (A) Principal component analysis (PCA) scores plot and (B) loadings plot of ^{1}H NMR spectral data obtained from M1 (blue), M2 (red), and M3 (green)

This analysis revealed a distinct cluster formation, effectively separating each class of *M. moribidii*. M1 and M2 were in the same cluster within the right quadrant of the PCA scores plot, indicating that they share a similar chemical profile (Figure 2A). As anticipated, the separation between these age classes was primarily attributed to variations in amino acid content and other metabolites overlapping with the glucose region, such as trigonelline, fatty acid, inosinic acid or inosine monophosphate (IMP) and 4-hydroxyphenylacetic acid (4-HPA) (Figure 2B). According to the PCA scores plot, M1 and M2 overlapped, suggesting similar metabolite features between these two groups. The PCA loadings plot indicated that M3 shares the same metabolites as M1, but the metabolites of M3 are presented at lower concentrations, as evidenced by the lower intensity of their chemical shifts compared to the others. The relative quantification of identified metabolites was performed to determine the significant differences between the different classes (Supplementary Table 1). According to the results, the concentrations of M1 and M2 metabolites are not significantly different, while the metabolites of M3 (mostly at low concentrations) are significantly different compared to M1 and M2. In addition, identifying other metabolites in M3 was challenging due to suppressing their signals in the NMR spectra by glucose signals and other metabolites overlapping with the glucose region. Therefore, comparing the two classes via OPLS-DA models was conducted to obtain a clearer metabolite profile of the different classes (M1 versus M2, M2 versus M3, and M1 versus M3).

The OPLS-DA models were conducted to investigate the significant difference between the different age classes of *M. moribidii.* CV-ANOVA and permutation tests were performed to validate the OPLS-DA models (Supplementary Figure 2-4). The model exhibited a distinct cluster formation, effectively separating the M1, M2 and M3. Interestingly, a trend within each age class of *M. moribidii* was observed, as depicted in the loading scatter plot of M1 and M2 (Figure 3A), where no significant cluster was observed in the 2D scores plot. This suggests that there is no significant difference between M1 and M2. When comparing three groups, the data becomes more complex, and the relationships between groups are

harder to interpret, especially if the models struggle to differentiate the classes due to similar metabolites in M1 and M2. Additionally, the p-value (< 0.05) based on the CV-ANOVA test further supports the finding that there is no significant difference between these two classes, as shown in Supplementary Figure 2. Jackknife error used in the OPLS-DA model refers to the estimation of model stability and generalizability by systematically leaving out one data point at a time during the analysis. In the context of an OPLS-DA scores plot, jackknife error helps assess the robustness of the model's ability to discriminate between groups. Some of the jackknife error bars are bigger than others in Figure 3 (A) (M1 versus M2) because certain data points may influence the model's performance more. Larger error bars suggest greater variability in the model's performance.

The OPLS-DA model explains the variation among compositions and their contribution to the discrimination pattern. Figure 3A shows the OPLS-DA scores plot for M1 (blue) versus M2 (red), while Figures 3B and 3C depict scores plots for M1 (blue) versus M3 (green) and M2 (red) versus M3 (green), respectively. Based on the OPLS-DA scores plots, discrimination of different ages of *M. moribidii* was achieved between M1 and M3 (Figure 3B), as well as M2 and M3 (Figure 3C), indicating the significant difference between M3 and other age classes. Based on the OPLS-DA loading column plots, most of the metabolites are shown to be higher in M1 and M2 compared to M3 (Supplementary Figures 3C and 4C). The results suggested that M1 and M2 are the best ages to be cultivated. The findings were also supported by the relative quantification of identified metabolites of M1, M2, and M3, as presented in Supplementary Table 1. Supplementary Figure 5 presents boxplots of metabolites from the three groups of *M. moribidii*.

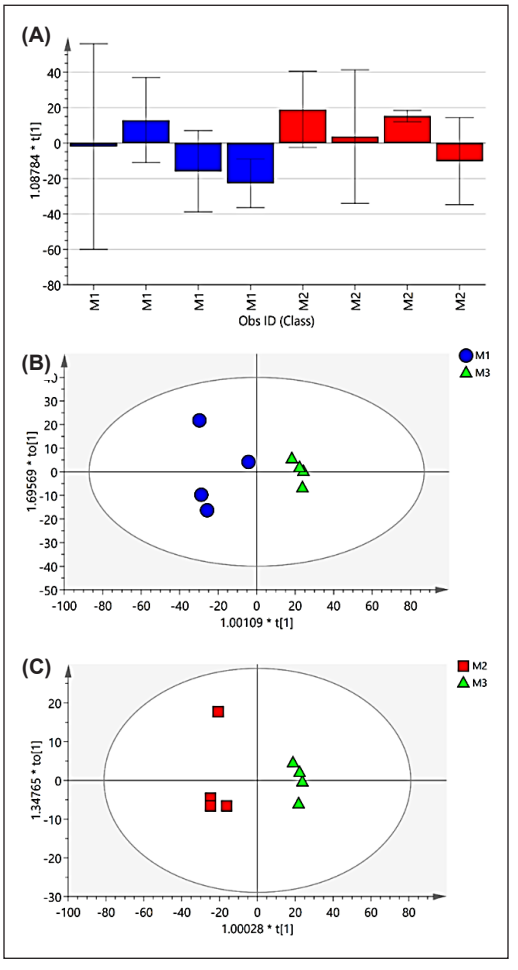

Figure 3. Orthogonal partial least squares discriminant analysis (OPLS-DA) scores plot of (A) M1 (blue) versus M2 (red), (B) M1 (blue) versus M3 (green), and (C) M2 (red) versus M3 (green)

A previous study found that harvest times influence polychaetes' chemical composition and metabolic variations

(Wijaya et al., 2024). Metabolites are more abundant during the hot season due to higher temperatures accelerating metabolism and supporting growth and reproduction. In contrast, the rainy season's reduced salinity and variable conditions may stress the polychaetes, lowering metabolic activity and metabolite production.

Metabolite Profile of Three Age Classes of *M. moribidii* Extract Based on LC-MS/MS Analysis

LC-MS/MS analysis was performed to better understand the metabolites present in *M. moribidii* at different ages. Since LC-MS/MS analysis is more sensitive than ^{1}H NMR analysis, a greater number of secondary metabolites are anticipated to be identified. This study used qualitative metabolite identification based on LCMS/MS analysis. The signal-to-noise (S/N) ratio was an essential factor for the analysis. Signals of metabolites with an S/N ratio below 1 (S/N ratio < 1) were not identified, as they were considered noise rather than meaningful data. This threshold ensures that only reliable and robust signals are included in the interpretation, minimising the risk of false positives due to background noise. Identification of metabolites was performed using the m/z and MS/MS fragmentations of interest compounds and comparing them with the m/z and MS/MS fragmentations of standard compounds available in the database. Nonetheless, a total of 36 compounds were tentatively identified from various age classes of *M. moribidii,* using LC-MS/MS, including organic acids, carbohydrates, phenolic, fatty acids and amino acids, with only one compound extra compared to ^{1}H NMR metabolomics. The proposed compounds for the three distinct age classes of *M. moribidii* are shown in Table 3*,* highlighting the differences observed in the presence or absence of these compounds.

Major identified metabolites of *M. moribidii* can be classified into primary and secondary metabolites. Primary metabolites refer to small chemical compounds such as organic acids, carbohydrates, phenolic, fatty acids, and amino acids that are directly involved in the growth, development, and reproduction of living organisms (Salam et al., 2023). These compounds are essential for maintaining normal physiological functions in the body. On the other hand, secondary metabolites are organic acids, carbohydrates, phenolics, fatty acids, and amino acids produced by modifying primary metabolites. These secondary metabolites are typically synthesised during the stationary phase of growth. Unlike primary metabolites, secondary metabolites do not play a direct role in growth, development, or reproduction (Bruce, 2022). Instead, they often serve ecological functions such as defence mechanisms and can exhibit properties such as antibiotics, antimicrobial, antifungal, anticancer, and antiviral (Izzati et al., 2021).

As depicted in Table 3, sucrose was detected in M1, M2 and M3 samples, with a retention time (RT) of 13.65 and a mass-to-charge ratio (m/z) of 341.1069. Sucrose and glucose were also identified in ^{1}H NMR spectra of *M. moribidii* of different ages. Sucrose,

a simple carbohydrate with low reactivity, plays essential roles in both plants and animals. Sucrose is commonly used in marine worms to store energy. Like many other organisms, marine worms require energy to perform biological processes such as movement, growth, and reproduction (Ulu et al., 2021). Marine worms can consume sucrose directly from their surroundings or by breaking down other organic matter. Once ingested, sucrose can be broken down into monosaccharides (glucose) that are then utilised in cellular respiration to generate ATP (adenosine triphosphate), the primary energy currency of cells (Khowala et al., 2008).

Cyclo (Pro-Val) is a cyclic dipeptide composed of proline and valine. It is found in sponges, molluscs, and some marine bacteria and can perform a variety of functions (Zeng et al., 2023). These organisms produce and utilise Cyclo (Pro-Val) as part of their metabolic processes. These compounds may play a role in osmoregulation, helping marine worms adapt to changes in salinity and other environmental conditions. In some cases, Cyclo (Pro-Val) can provide nitrogen or other nutrients to marine organisms, contributing to their growth and development. Based on its known biological activities, Cyclo (Pro-Val) is anticipated to contribute to various physiological processes that support the health and adaptation of marine worms in their aquatic environment (Bojarska et al., 2021).

L-tyrosine is a natural protein building block presented in M1 and M3 samples while absent in M2. This observation suggests that, rather than being a naturally occurring substance in M2, the source of L-tyrosine may be a nutrient found in sediment that the organism uses as sustenance. Since L-tyrosine is an amino acid that the body can synthesise, it is considered a non-essential amino acid (Lopez & Mohiuddin, 2024).

In contrast, L-phenylalanine is presented only in M2, indicating that the nutrient content in *M. moribidii* extract primarily originates from the soil. According to Aliu et al. (2018), phenylalanine and tyrosine differ primarily because the former is an essential amino acid while the latter is a non-essential amino acid. However, the amino acids of acetylglucosamine, which are well recognised for their structural roles at the cell surface, were only found in M3 at a m/z of 266.0891. It is a crucial part of the extracellular matrix found in animal cells, the fungus chitin, and the bacterium peptidoglycan. Furthermore, N-alpha-acetyl-L-lysine, a derivatised alpha amino acid, is identified at m/z of 187.1088 in M2 and M3. It is the biologically accessible N-terminal capped form of L-lysine, an alpha amino acid prevalent in proteins.

Interestingly, the only phenolic molecule identified in *M. moribidii* was 2-methoxy-4-acetylphenyl-1-O-β-D-apiofuranosyl-(1''→6')-β-D glucopyranoside and specifically found in M2 sample. It belongs to a group of natural products known as glycosides, commonly occurring as β-D-glucosides, which are presented in various plant pigments such as anthocyanins. Phenolic glycosides have been newly identified in *M. moribidii,* marking the first representative of their presence in this species. Since glycosides are

Table 3
Identification of three different age classes of Marphysa moribidii

No.	RT (min)	m/z	Adduct	Neutral mass (Da)	MS/MS fragment ions	Mass error (ppm)	Tentative compound	Availability		
								M1	M2	M3
1	0.62	367.1060	$[M-H]^-$	368.1132	353, 331	6.8	3-Feruloylquinic acid	x	/	x
2	0.93	180.0667	$[M-H]^-$	181.0739	163, 202	0.2	L-Tyrosine	/	x	/
3	0.94	405.1040	$[M+HCOO]^-$	360.1058	322, 324,163,180	0.4	Glucosyringic acid	/	/	/
4	1.23	266.0891	$[M+HCOO]^-$	221.0909	150	3.5	Acetylglucosamine	x	x	/
5	1.73	164.0717	$[M-H]^-$	165.0790	201	0.0	L-Phenylalanine	x	/	x
6	1.83	187.1088	$[M-H]^-$	188.1160	187	-0.3	N-alpha-acetyl-L-lysine	x	/	/
7	3.76	459.1504	$[M-H]^-$	460.1577	258	-0.9	2-Methoxy-4-acetylphenol 1-O-α-L-rhamnopyranosyl-(1''→6')-β-D-glucopyranoside	x	/	x
8	3.76	459.1504	M-H	460.1577	244, 375	-0.9	2-Methoxy-4-acetylphenyl-1-O-β-D-apiofuranosyl-(1''→6')-β-D-glucopyranoside	x	/	x
8	4.18	593.2191	$[M-H]^-$	594.2263	227, 439	-8.2	Pseudolaric acid B O-β-D-glucopyranoside	x	/	x
9	5.43	241.1194	$[M+HCOO]^-$	196.1212	197	0.0	Cyclo(Pro-Val)	/	/	/
10	5.91	255.0882	$[M+HCOO]^-$	210.0900	212	2.9	Ethyl-5-ethoxy-2-hydroxy benzoate	x	/	/
11	13.38	237.1112	$[M+HCOO]^-$	192.1130	197	-8.7	Phenylethyl butanoic acid	/	x	/
12	13.65	341.1069	$[M-H]^-$	342.1142	171	-5.9	Sucrose	/	/	/
13	15.59	417.1560	$[M-H]^-$	418.1633	415, 180	1.2	Pseudolaric acid C2	/	/	/
14	15.85	267.1968	$[M-H]^-$	268.2040	267	0.7	13-Hydroxy-9,11-hexadecadienoic acid	/	x	x
15	15.98	313.2384	$[M-H]^-$	314.2456	201, 313, 96	-0.3	Dibutyl sebacate	/	/	/
16	16.10	361.1634	$[M-H]^-$	362.1707	304,220	1.2	Thyrotropin Releasing Hormone	/	/	/
17	16.99	311.2231	$[M+HCOO]^-$	266.2249	171, 293, 193	1.0	Methyl 7,10-hexadecadienoic acid	/	/	/
18	17.00	339.2541	$[M+HCOO]^-$	294.2559	315, 319, 321	0.0	9,12-Octadecadienoic acid methylester	/	/	/
19	17.00	339.2541	$[M+HCOO]^-$	294.2559	319,199, 321	0.0	10,13-Ethyl octadecadienoic acid	x	/	/
20	17.28	293.2121	$[M-H]^-$	294.2193	207,171	-0.5	(E,E)-9-Oxooctadeca-10,12-dienoic acid	x	/	/

Table 3 *(continue)*

No.	RT (min)	m/z	Adduct	Neutral mass (Da)	MS/MS fragment ions	Mass error (ppm)	Tentative compound	Availability		
21	17.28	379.2102	$[M+HCOO]^-$	334.2120	255, 193	-6.5	Di (2-ethyl butyl) phthalic acid	/	/	/
22	17.80	335.2223	$[M+HCOO]^-$	290.2241	295	-1.5	6,9-Octadecadiynoic acid, methyl ester	x	/	/
23	17.91	253.1807	$[M-H]^-$	254.1879	233	-1.0	9-Hydroxy-10,12-pentadecadienoic acid	x	/	/
24	17.98	275.2015	$[M-H]^-$	276.2088	275	-0.4	Stearidonic acid	x	/	/
25	17.99	315.2540	$[M-H]^-$	316.2612	297	-0.4	Dihydroxy stearic acid	/	/	/
26	18.21	341.2690	$[M+HCOO]^-$	296.2708	229	-2.0	Methyl oleic acid	x	/	x
27	18.41	295.2278	$[M-H]^-$	296.2351	277, 195	-0.2	Coronaric acid	x	/	/
28	18.64	277.2171	$[M-H]^-$	278.2244	195	-0.7	γ-Linoleic acid	x	/	/
29	19.08	297.2441	$[M-H]^-$	298.2514	343	2.1	Ricinoleic acid	x	/	/
30	21.81	281.2488	$[M-H]^-$	282.2560	281, 282	0.6	Elaidic acid	x	/	/
31	21.82	281.2491	$[M-H]^-$	282.2564	281	1.9	(E)-9-Octadecenoic acid	x	/	x
32	23.46	337.3113	$[M-H]^-$	338.3186	337	0.3	Erucic acid	x	/	/
33	24.35	383.3529	$[M-H]^-$	384.3602	211, 247, 255	-0.4	α-Hydroxy tetracosanic acid	x	/	/
34	26.25	744.5538	$[M+HCOO]^-$	745.5611	223	-1.4	Phosphatidyl ethanolamine	x	x	/
35	328.26	373.2589	$[M+HCOO]^-$	328.2607	353	-1.9	9,12-Dihydroxy-15-nonadecenoic acid	x	/	x

/ Presence
X Absence

classified as secondary metabolites, they can act as chemical defences against predators, and this compound often possesses antimicrobial properties, which help to protect marine invertebrates from infections and diseases in their marine environment (Choudhary et al., 2017).

Fatty acid esters, which are derivatives of carboxylic acid, are also largely found in *M. moribidii* at different ages, as presented in Table 3. Methyl oleic acid and phenylethyl butanoic acid are fatty acid esters found only in M2 samples at m/z of 341.2690 and 237.1112, respectively. Methyl oleic acid results from the condensation of oleic acid with methanol and occurs naturally in various fats and oils of both animal and plant origin. Like other fatty acids, methyl oleic acid can serve as a source of energy when metabolised by the organism, and it is an integral component of cell membranes, providing stability and fluidity (Ali & Szabó, 2023). At the same time, phenylethyl butanoic acid was not classified in the phenyl group and contained a hydrogen atom in its molecular structure. Phenylethyl butanoic acid is an aromatic compound with a butanoic acid side chain and a phenethyl group. Aromatic compounds frequently serve as signalling molecules in intra- and interspecies communication. They can convey information about mating, territorial boundaries, or danger, while some aromatic compounds can influence behaviours such as feeding or social interactions among marine invertebrates (Elgar, 2019).

Stearidonic acid, which is synthesised from alpha-linolenic acid and γ-linoleic acid (LA), was detected at m/z 275.2015 and 277.2171 in both M1 and M2, respectively. LA is an essential nutrient with important physiological functions in various organisms. However, the mechanism of LA synthesis differs among species, as observed in studies involving insects, nematodes, and pulmonates (Malcicka et al., 2018). Ricinoleic acid has been found in M2 and M3 at m/z 297.2441, indicating extensive metabolism in the rumen and tissues, while coronaric acid at m/z 295.2278, is produced by cells and tissues of various mammalian species, including humans, through linoleic acid metabolism. These findings are supported by studies conducted by Alves et al. (2017) and Konkel and Schunck (2011). Furthermore, 9,12-octadecadienoic acid methylester, which has antibacterial properties, was found in all age classes of *M. moribidii* (M1, M2, and M3) at m/z 294.2559 (Rahman et al., 2014). Additionally, according to a study by Gheda and Ismail (2020), methyl 7,10-hexadecanoic at m/z 311.2231, which was also detected in all age classes of *M. moribidii* and classified as a linoleic acid ester, has demonstrated antioxidant, anti-inflammatory, and hypocholesterolemic characteristics.

Additional substances found in M1, M2, and M3 included the peptide thyrotropin-releasing hormone (TRH), a peptide which is mostly generated by brain neurons. Thyroid-stimulating hormone (TSH), which regulates the thyroid axis through neurons in the hypothalamus, is secreted by the anterior pituitary gland in animals in response to stimulation by TRH (Charli et al., 2020). Although TRH was first identified in relation to TSH release,

it has a variety of impacts on different species (Galas et al., 2009). Phthalates are another group of compounds found in all age classes of *M. moribidii*. They are naturally occurring, bioactive substances that plants, bacteria, fungi produce, and other organisms (Huang et al., 2021). On the other hand, only M3 showed signs of phosphatidylethanolamines, which is likely related to *M. moribidii*'s elderly age. Phosphotidylethanolamines, which make up approximately 25% of phospholipids, are essential components in all living cells (Calzada et al., 2016). They are widely distributed in brain tissue, neurons, and the spinal cord in humans and account for 45% of phospholipids. They serve critical roles in several biological pathways, including membrane fusion, cell division, and membrane curvature (Vance & Tasseva, 2013; Imbs et al., 2021).

Compound Distribution in Different Age Classes of *M. moribidii*

The Venn diagram depicts unique compounds that have been discovered in different age classes of *M. moribidii* (designated by M1, M2, and M3), and Figure 4 summarises the distribution of compounds. According to the Venn diagram, all three different age classes of *M. moribidii* share a common set of 41 compounds identified through a combination of LC-MS/MS and NMR metabolite analysis. However, five metabolites appear in both datasets, eliminating these duplicates. The distribution of metabolites was constructed in that way to ensure accuracy and precise analysis by eliminating duplicates and reducing redundancy. After data acquisition, metabolites identified by both LC-MS/MS and NMR are compared for overlap. Duplicate entries are removed when both methods detect the same compound to ensure unique metabolite representation in the final dataset. Redundancy occurs as both techniques can identify the same metabolites, including organic acids, carbohydrates, phenolics, fatty acids and amino acids.

Interestingly, the M1 variety exhibits one unique compound, while the M2 and M3 varieties have seven and two unique compounds, respectively. Relative quantification of identified metabolites based on NMR analysis indicates the metabolite variations in different classes of polychaetes, showing that M3 has fewer metabolites compared to M1 and M3 (Supplementary Table 1). Specifically, only a single, distinctive compound of 13-hydroxy-9,11-octadecadienoic acid was identified in M1. This monohydroxy fatty acid plays a significant role in marine

Figure 4. Venn diagram showing compound distribution in different age classes of *M. moribidii*

invertebrates. Previous research has demonstrated the notable antifungal activity of unsaturated hydroxy fatty acids with hydroxylation at the C9–C13 positions in a C18 chain (Guimarães & Venâncio, 2022). Furthermore, hydroxy fatty acids such as 11-HEPE and 15-HEPE have been found in diatoms through investigations on lipoxygenase pathways, suggesting their involvement in a variety of biological activities (Ruocco et al., 2020). According to these findings, 13-hydroxy-9,11-octadecadienoic acid and related compounds may support several various physiological and ecological processes in marine invertebrates, including signalling and defence systems.

Interestingly, M2 is categorised as having the greatest number of unique metabolites found compared to M1 and M3, as it shows seven distinct metabolites. The first metabolite identified in M2 is L-phenylalanine. Limited information is available regarding the specific function of L-phenylalanine in marine invertebrates. However, research indicates that phenylalanine plays important roles in regulating the capacity of intestinal immunity, antioxidants, and apoptosis in fish, including largemouth bass and gilthead seabream. In addition, phenylalanine is essential for synthesising proteins, catecholamines, and melanin (Salamanca et al., 2021; Yi et al., 2023).

The next compound discovered in M2 is 2-methoxy-4-acetylphenol 1-O-α-L-rhamnopyranosyl-(1''→6')-β-D-glucopyranoside, an aromatic compound classified as phenylpropanoid glycoside. Phenylpropanoid glycosides are known for their wide range of biological activities, including antioxidant, anti-inflammatory, and antimicrobial properties (Skalski et al., 2021). Consequently, this compound holds the potential to contribute to the biological activities associated with marine invertebrates. Another compound identified in M2 is 2-methoxy-4-acetylphenyl-1-O-β-D-apiofuranosyl-(1''→6')-β-D-glucopyranoside, a complex sugar molecule with recognised activities in marine invertebrates (D'Abrosca et al., 2010). Depending on the specific species and its presence in their tissues or secretions, this compound may serve a variety of functions in marine invertebrates. In general, sugar molecules are essential to many biological functions, including cell signalling, energy storage, and structural support (Rolland et al., 2002).

Additionally, M2 contains pseudolaric acid β-O-beta-D-glucopyranoside, classified as a rifamycin, and has anti-tuberculosis properties. According to Li et al. (2020), pseudolaric acid has been demonstrated to exhibit a variety of biological functions, for instance, serving as an antifungal agent. M2 also contains a fatty acid ester of methyl oleic acid that shares functional similarities with oleic acid, which is recognised for its diverse activities in various roles, including being a carboxylesterase inhibitor and a metabolite in different organisms (Ruiz et al., 2022). Octadecenoic acid is another next-generation metabolite found in M2. Octadecenoic acid content changes according to the species and habitat of the marine invertebrate. It is also found in the phospholipids of *Holothuria mexicana* and is a trace element in *Kamptosoma abyssale*, an abyssal species (Barnathan, 2009).

9,12-dihydroxy-15-nonadecenoic acid, a chemical compound present in various marine invertebrates, is the final distinct metabolite found in M2. Its occurrence in these organisms raises the possibility that it plays a part in their biology and defence systems. Sponge-like marine invertebrates depend on humoral and cellular immunity as part of their innate immune systems (Sperstad et al., 2011). The existence of 9,12-dihydroxy-15-nonadecenoic acid in marine invertebrates suggests a potential contribution to their innate immune system and plays a role in protecting them against various pathogens, even though it is not specifically discussed in the context of these organisms' defence mechanisms.

The old age class of *M. Moribidii* (M3) shows the presence of two distinct chemicals where the first compound identified is acetylglucosamine. According to Riemann and Azam (2002), acetylglucosamine is known as an important constituent of structural polymers found in bacteria, plants, and animals, including various marine invertebrates such as cuttlefish, crab, and lobster, as well as fungi and algae. The subsequent compound identified in M3 is phosphatidylethanolamines (PE), which plays a crucial role in marine invertebrates as a major structural lipid in cell membranes. Furthermore, ethanolamine-containing special glycerophospholipid plasmalogens, which are prevalent in several marine invertebrates, have been associated with benefits for age-associated diseases (Yamashita et al., 2023). Consequently, PE plays a crucial part in the composition and operation of marine invertebrates' cell membranes. In summary, *M. moribidii* has distinct fatty acid, amino acid, and phospholipid components at both the young (M1) and old (M3) ages. Interestingly, *M. moribidii* (M2) has a higher concentration of different substances in its middle age, such as amino acids, fatty acids, fatty acid esters, and phenylpropanoid glycoside.

As far as we know, no research has been conducted on the metabolite profile of various ages of marine worms. Among the most popular model organisms to investigate the molecular mechanisms of ageing are the nematodes of *Caenorhabditis elegans* due to their short lifespan and ease of cultivation in the laboratory (Balashova et al., 2022). Copes et al. (2015) studied global quantification of metabolite and protein levels in young and aged nematodes of *C. elegans* using mass spectrometry, which successfully identified 186 metabolites. The metabolomics data show that as *C. elegans* ages, the levels of free fatty acid and sorbitol content increase, while those of specific purine and pyrimidine metabolites, free hydrophobic amino acids and altered S-adenosyl methionine metabolism decrease, and a shift in cellular redox balance.

Figure 5 summarises the proposed metabolic pathway involved in *M. moribidii*. According to the results, there are four important metabolic pathways in *M. moribidii:* phenylalanine, tyrosine and tryptophan biosynthesis, phenylalanine metabolism, taurine and hypotaurine metabolism, and beta-alanine metabolism. This pathway analysis highlights significant metabolites, particularly emphasising primary metabolites that play essential roles in the metabolism of *M. moribidii.*

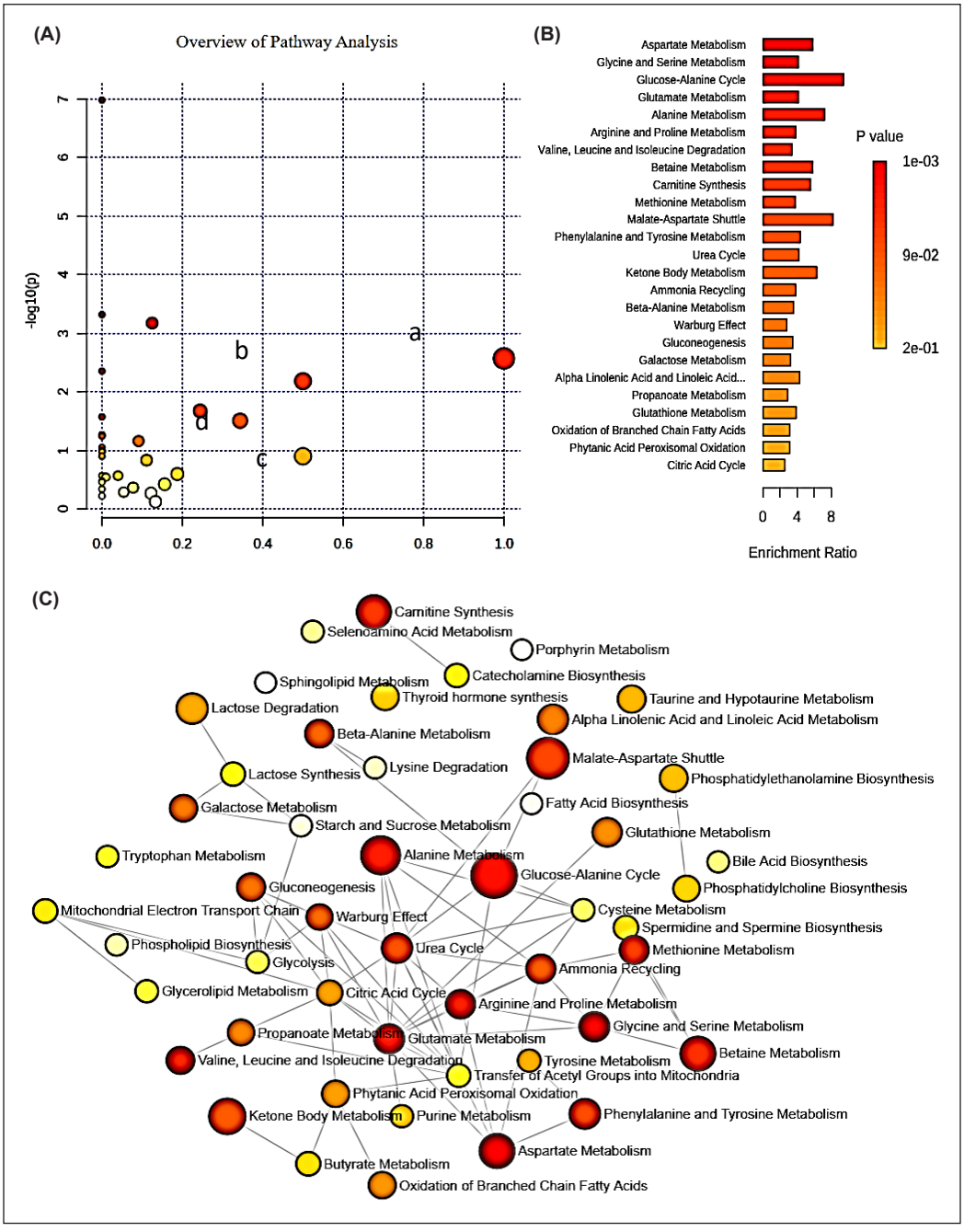

Figure 5. Summary of pathway analysis determined using Metaboanalyst. (A) Pathway impact: (a) Phenylalanine, tyrosine and tryptophan biosynthesis; (b) Phenylalanine metabolism; (c) Taurine and hypotaurine metabolism; (d) beta-Alanine metabolism. (B) Metabolite sets enrichment overview and MetaMapp visualisation of metabolomic data highlighting the differential metabolic regulation. (C) MetaMapp graphs in Cytoscape showed much clearer metabolic modularity and complete content visualisation compared to conventional biochemical mapping approaches

Pathway analysis using MetaboAnalyst typically provides an overview of the key metabolic pathways that are most relevant to *M. moribidii*. This type of analysis integrates metabolite data and maps them to know their metabolic pathways, allowing for a broader understanding of the biochemical processes occurring within the organism. In a MetaMapp graph, nodes represent metabolites like glucose, amino acids, or lipids. At the same time, the edges and the lines connecting the nodes show the relationships or interactions between metabolites. These relationships can include biochemical conversions, where enzymes change one metabolite into another or connect between different metabolic modules. The graph can be adjusted to show how metabolites and pathways are linked, with edges and nodes clearly showing which metabolites are involved in which pathways and how they are grouped together. The metabolic pathways in Figure 5C show the overview of the general metabolite involved in *M. moribidii*.

CONCLUSION

We observed a comprehensive spectrum of metabolite profiles in marine worms, *M. moribidii*, from various age classes using NMR and LC-MS/MS analysis, including organic acids, carbohydrates, phenolics, fatty acids, and amino acids. *M. moribidii*'s middle age (M2) classes have the most identified chemicals (62 metabolites) when compared to the young (M1) and old age (M3) classes. The most noticeable discovery from this study is that M2 has the maximum number of seven distinct metabolites composed of fatty acid, amino acid, phenylpropanoid glycoside, and fatty acid esters compared to the young and old classes of *M. moribidii*. M2 unique metabolites might contribute to a variety of biological activities, including antioxidant, anti-inflammatory, antibacterial, and defence and immunological systems. These data indicate that discrepancies in age classifications of *M. moribiii* result in diverse metabolite profiles, with not all metabolites present in different age classes of *M. moribiii*. Overall, this study improves our understanding of *M. moribidii*, an intriguing annelid species, by emphasising the significance of metabolomics in identifying the numerous metabolic pathways associated with its various age classes. This study's findings shed light on the physiology and ecology of metabolic variability, establishing the groundwork for future research into the genetic and biochemical mechanisms behind the observed changes in *M. moribidii* metabolism.

ACKNOWLEDGEMENT

The author acknowledges the support of the Ministry of Higher Education (MOHE) Malaysia through the Fundamental Research Grant Scheme (FRGS/1/2020/STG02/UMT/02/1). We also thank Universiti Malaysia Terengganu for their generous support.

REFERENCES

Ali, O., & Szabó, A. (2023). Review of eukaryote cellular membrane lipid composition, with special attention to the fatty acids. *International Journal of Molecular Sciences, 24*(21), Article 15693. https://doi.org/10.3390/ijms242115693

Aliu, E., Kanungo, S., & Arnold, G.L. (2018). Amino acid disorders. *Annals of Translational Medicine, 6*(24), 471–471. https://doi.org/10.21037/atm.2018.12.12

Alves, S. P., Araujo, C. M., Queiroga, R. C., Madruga, M. S., Parente, M. O. M., Medeiros, A. N., & Bessa, R. J. B. (2017). New insights on the metabolism of ricinoleic acid in ruminants. *Journal of Dairy Science, 100*(10), 8018–8032. https://doi.org/10.3168/jds.2017-13117

Balashova, E. E., Maslov, D. L., Trifonova, O. P., Lokhov, P. G., & Archakov, A. I. (2022). Metabolome profiling in aging studies. *Biology, 11*, Article 1570. https://doi.org/10.3390/biology11111570

Barnathan, G. (2009). Non-methylene-interrupted fatty acids from marine invertebrates: Occurrence, characterization and biological properties. *Biochimie, 91*(6), 671–678. https://doi.org/10.1016/j.biochi.2009.03.020

Bojarska, J., Mieczkowski, A., Ziora, Z., Skwarczynski, M., Toth, I., Shalash, A. O., Parang, K., El-Mowafi, S. A., Mohammed, E. H. M., Elnagdy, S., Alkhazindar, M., & Wolf, W. M. (2021). Cyclic dipeptides: The biological and structural landscape with special focus on the anti-cancer proline-based scaffold. *Biomolecules*, *11*(10), Article 1515. https://doi.org/10.3390/biom11101515

Bruce, S. O. (2022). Secondary metabolites from natural products. In R. Vijayakumar & S. S. S. Raja (Eds.), Secondary Metabolites - Trends and Reviews (pp. 51-70). IntechOpen. https://doi.org/10.5772/intechopen.102222

Calzada, E., Onguka O., & Claypool, S. M. (2016). Phosphatidylethanolamine metabolism in health and disease. *International Review of Cell and Molecular Biology, 321*, 29–88. https://doi.org/10.1016/bs.ircmb.2015.10.001

Capa, M., & Hutchings P. (2021). Annelid diversity: Historical overview and future perspectives. *Diversity, 13*(3), 1–14. https://doi.org/10.3390/d13030129

Charli, J. L., Rodríguez-Rodríguez, A., Hernández-Ortega, K., Cote-Vélez, A., Uribe, R. M., Jaimes-Hoy, L., & Joseph-Bravo, P. (2020). The thyrotropin-releasing hormone-degrading ectoenzyme, a therapeutic target? *Frontiers in Pharmacology, 11*, 1–21. https://doi.org/10.3389/fphar.2020.00640

Choudhary, A., Naughton, L. M., Montánchez, I., Dobson, A. D. W., & Rai, D. K. (2017). Current status and future prospects of marine natural products (MNPs) as antimicrobials. *Marine Drugs*, *15*(9), Article 272. https://doi.org/10.3390/md15090272

Copes, N., Edwards, C., Chaput, D., Saifee, M., Barjuca I., Nelson, D., Paraggio, A., Saad, P., Lipps, D., Stevens, S. M., & Bradshaw, P. C. (2015). Metabolome and proteome changes with aging in *Caenorhabditis elegans*. *Experimental Gerontology, 72*, 67–84. https://doi.org/10.1016/j.exger.2015.09.013

D'Abrosca, B., Fiorentino, A., Ricci, A., Scognamiglio, M., Pacifico, S., Piccolella, S., & Monaco, P. (2010). Structural characterization and radical scavenging activity of monomeric and dimeric cinnamoyl glucose

esters from *Petrorhagia velutina* leaves. *Phytochemistry Letters, 3*(1), 38–44. https://doi.org/10.1016/j.phytol.2009.11.001

Elgar, M. A. (2019). Chemical signaling: Air, water, and on the substrate. *Encyclopedia of Animal Behavior*, *1*, 462 – 473. https://doi.org/10.1016/B978-0-12-809633-8.90718-0

Emwas, A. H., Roy, R., McKay, R. T., Tenori, L., Saccenti, E., Gowda G. A. N., Raftery, D., Alahmari, F., Jaremko, L., Jaremko, M., & Wishart, D. S. (2019). NMR spectroscopy for metabolomics research. *Metabolites, 9*(7), Article 123. https://doi.org/10.3390/metabo9070123

Galas, L., Raoult, E., Tonon, M. C., Okada, R., Jenks, B. G., Castaño, J. P., Kikuyama, S., Malagon, M., Roubos, E. W., & Vaudry, H. (2009). TRH acts as a multifunctional hypophysiotropic factor in vertebrates. *General and Comparative Endocrinology, 164*(1), 40–50. https://doi.org/10.1016/j.ygcen.2009.05.003

Gathungu, R. M., Kautz, R., Kristal, B. S., Bird, S. S., & Vouros, P. (2020). The integration of LC-MS and NMR for the analysis of low molecular weight trace analytes in complex matrices. *Mass Spectrometry Reviews, 39*(1-2), 35–54. https://doi.org/10.1002/mas.21575

Gheda, S. F., & Ismail, G. A. (2020). Natural products from some soil cyanobacterial extracts with potent antimicrobial, antioxidant and cytotoxic activities. *Anais da Academia Brasileira de Ciências, 92*(2), 1–18. https://doi.org/10.1590/0001-3765202020190934

Glasby, C. J., & Timm, T. (2008). Global diversity of polychaetes (Polychaeta; Annelida) in freshwater. In E. V. Balian, C. Lévêque, H. Segers, & K. Martens (Eds.), *Freshwater Animal Diversity Assessment* (pp. 107–115). Springer. https://doi.org/10.1007/978-1-4020-8259-7_13

Glasby, C. J., Erséus, C., & Martin, P. (2021). Annelids in extreme aquatic environments: Diversity, adaptations and evolution. *Diversity*, *13*(2), Article 98. https://doi.org/10.3390/d13020098

Górska, B., Gromisz, S., & Włodarska-Kowalczuk, M. (2019). Size assessment in polychaete worms - Application of morphometric correlations for common North Atlantic taxa. *Limnology and Oceanography: Methods, 17*(4), 254–265. https://doi.org/10.1002/lom3.10310

Guimarães, A., & Venâncio, A. (2022). The potential of fatty acids and their derivatives as antifungal agents: A review. *Toxins, 14*(188), 1–21. https://doi.org/10.3390/toxins14030188

Hassan, M. S. A., Elias, N. A., Hassan, M., Rahmah, S., Wan, I. W. I., & Harun, N. A. (2023). Polychaeta-mediated synthesis of gold nanoparticles: A potential antibacterial agent against Acute Hepatopancreatic Necrosis Disease (AHPND)–causing bacteria, *Vibrio parahaemolyticus*. *Heliyon*, *9*(2023)**,** Article e21663. https://doi.org/10.1016/j.heliyon.2023.e21663

Huang, L., Zhu, X., Zhou, S., Cheng, Z., Shi, K., Zhang, C., & Shao, H. (2021). Phthalic acid esters: Natural sources and biological activities. *Toxins, 13*(7), Article 495. https://doi.org/10.3390/toxins13070495

Idris, I., & Arshad, A. (2013). Checklist of polychaetous annelids in Malaysia with redescription of two commercially exploited species. *Asian Journal of Animal and Veterinary Advances*, *8*(3), 409-436.

Idris, I., & Hutchings, P. (2014). Description of a new species of *Marphysa* Quatrefages, 1865 (Polychaeta: Eunicidae) from the west coast of Peninsular Malaysia and comparisons with species from *Marphysa* Group A from the Indo-West Pacific and Indian Ocean. *Memoirs of Museum Victoria, 71*, 1447–2554. https://doi.org/10.24199/j.mmv.2014.71.11

Imbs, A. B., Ermolenko, E. V., Grigorchuk, V. P., Sikorskaya, T. V., & Velansky, P. V. (2021). Current progress in lipidomics of marine invertebrates. *Marine Drugs, 19*(12), Article 660. https://doi.org/10.3390/md19120660

Izzati, F., Warsito, M. F., Bayu, A., Prasetyoputri, A., Atikana, A., Sukmarini, L., Rahmawati, S. I., & Putra, M. Y., (2021). Chemical diversity and biological activity of secondary metabolites isolated from Indonesian marine invertebrates. *Molecules, 26*(7), Article 1898. https://doi.org/10.3390/molecules26071898

Khowala, S., Verma, D., & Banik, S. P., (2008). Biomolecules: Introduction, structure & function. *Indian Institute of Chemical Biology,* 3–92.

Konkel, A., & Schunck, W.H. (2011). Role of cytochrome P450 enzymes in the bioactivation of polyunsaturated fatty acids. *Biochimica et Biophysica Acta (BBA) – Proteins and Proteomics, 1814*, 210–222. https://doi.org/10.1016/j.bbapap.2010.09.009

Li, Z., Yin, H., Chen, W., Jiang, C., Hu, J., Xue, Y., Yao, D., Peng, Y., & Hu, X. (2020). Synergistic effect of pseudolaric acid b with fluconazole against resistant isolates and biofilm of candida tropicalis. *Infection and Drug Resistance, 13*, 2733–2743. https://doi.org/10.2147/IDR.S261299

Lopez, M. J., & Mohiuddin, S. S. (2024). *Biochemistry, Essential Amino Acids*. StatPearls Publishing.

Malcicka, M., Visser, B., & Ellers, J. (2018). An evolutionary perspective on linoleic acid synthesis in animals. *Evolutionary Biology, 45*(1), 15–26. https://doi.org/10.1007/s11692-017-9436-5

Marion, D. (2013). An introduction to biological NMR spectroscopy. *Molecular & Cellular Proteomics, 12*(11), 3006–3025. https://doi.org/10.1074/mcp.O113.030239

Moco, S. (2022). Studying metabolism by NMR-based metabolomics. *Frontiers in Molecular Biosciences, 9*, 1–12. https://doi.org/10.3389/fmolb.2022.882487

Occhioni, G. E., Brasil, A., & Araújo, A. F. (2009). Morphometric study of Phragmatopoma caudata (Polychaeta: Sabellida: Sabellariidae). *Zoologia (Curitiba)*, *26*, 739-746.

Patel, M. K., Pandey, S., Kumar, M., Haque, M. I., Pal, S., & Yadav, N. S. (2021). Plants metabolome study: Emerging tools and techniques. *Plants, 10*(11), 1–24. https://doi.org/10.3390/plants10112409

Pei, A. U. E., Huai, P. C., Masimen, M. A. A., Wan, I. W. I., Idris, I., & Harun, N. A. (2020). Biosynthesis of gold nanoparticles (AuNPs) by marine baitworm *Marphysa moribidii* Idris, Hutchings and Arshad 2014 (Annelida: Polychaeta) and its antibacterial activity. *Advances in Natural Sciences: Nanoscience and Nanotechnology, 11*(1), Article 015001. https://doi.org/10.1088/2043-6254/ab6291

Rahman, M. M., Ahmad, S. H., Mohamed, M. T. M., & Rahman, M. Z. A. (2014). Antimicrobial compounds from leaf extracts of *Jatropha curcas, Psidium guajava*, and *Andrographis paniculata*. *The Science World Journal, 2014*, Article 35240. https://doi.org/10.1155/2014/635240

Rapi, H. S., Soh, N. A. C., Azam, N. S. M., Maulidiani, M., Assaw, S., Haron, M. N., Ali A. M., Idris, I., & Ismail, W. I. W. (2020). Effectiveness of aqueous extract of marine baitworm *Marphysa moribidii* Idris, Hutchings and Arshad, 2014 (Annelida, Polychaeta), on acute wound healing using Sprague Dawley rats. *Evidence-Based Complementary and Alternative Medicine, 2020*, Article 408926. https://doi.org/10.1155/2020/1408926

Riemann, L., & Azam, F. (2002). Widespread N-acetyl-D-glucosamine uptake among pelagic marine bacteria and its ecological implications. *Applied and Environmental Microbiology, 68*(11), 5554–5562. https://doi.org/10.1128/AEM.68.11.5554-5562.2002

Rolland, F., Moore, B., & Sheen, J. (2002). Sugar sensing and signalling in plants. *The Plant Cell*, *14*(1), 185–205. https://doi.org/10.1105/tpc.010455.S186

Rosman, N. S. R., Harun, N. A., Idris I., & Ismail, W. I. W. (2020). Eco-friendly silver nanoparticles (AgNPs) fabricated by green synthesis using the crude extract of marine polychaete, *Marphysa moribidii*: Biosynthesis, characterisation, and antibacterial applications. *Heliyon*, *6*(11), Article e05462. https://doi.org/10.1016/j.heliyon.2020.e05462

Rosman, N. S. R., Masimen, M. A. A., Harun, N. A., Idris, I., & Ismail, W. I. W. (2021). Biogenic silver nanoparticles (AgNPs) from *Marphysa moribidii* extract: Optimization of synthesis parameters. *International Journal of Technology, 12*(3), 635–648. https://doi.org/10.14716/ijtech.v12i3.4303

Ruiz, A. J. C., Boushehri, M. A. S., Phan, T., Carle, S., Garidel P., Buske, J., & Lamprecht, A. (2022). Alternative excipients for protein stabilization in protein therapeutics: Overcoming the limitations of polysorbates. *Pharmaceutics, 14*(12), Article 2575. https://doi.org/10.3390/pharmaceutics14122575

Ruocco, N., Nuzzo, G., d'Ippolito, G., Manzo, E., Sardo, A., Ianora, A., Romano, G., Iuliano, A., Zupo, V., Costantini, M., & Fontana, A. (2020). Lipoxygenase pathways in diatoms: Occurrence and correlation with grazer toxicity in four benthic species. *Marine Drugs, 18*(1), Article 66. https://doi.org/10.3390/md18010066

Salam, U., Ullah, S., Tang, Z. H., Elateeq, A. A., Khan, Y., Khan, J., Khan, A., & Ali, S. (2023). Plant metabolomics: An overview of the role of primary and secondary metabolites against different environmental stress factors. *Life, 13*(3), 1–25. https://doi.org/10.3390/life13030706

Salamanca, N., Giráldez, I., Morales, E., de La Rosa, I., & Herrera, M. (2021). Phenylalanine and tyrosine as feed additives for reducing stress and enhancing welfare in gilthead seabream and meagre. *Animals, 11*(1), 1–11. https://doi.org/10.3390/ani11010045

Skalski, B., Pawelec, S., Jedrejek, D., Rolnik, A., Pietukhov, R., Piwowarczyk, R., Stochmal, A., & Olas, B. (2021). Antioxidant and anticoagulant effects of phenylpropanoid glycosides isolated from broomrapes (*Orobanche caryophyllacea, Phelipanche arenaria*, and *P. ramosa*). *Biomedicine & Pharmacotheraphy, 139*, Article 111618. https://doi.org/10.1016/j.biopha.2021.111618

Sperstad, S. V., Haug, T., Blencke, H. M., Styrvold, O. B., Li, C., & Stensvåg, K. (2011). Antimicrobial peptides from marine invertebrates: Challenges and perspectives in marine antimicrobial peptide discovery. *Biotechnology Advances, 29*(5), 519–530. https://doi.org/10.1016/j.biotechadv.2011.05.021

Ulu, G., Semercioöz, A. S., & Özilgen, M. (2021). Energy storage and reuse in biological systems: Case studies. *Energy Storage*, *3*(5), 1–12. https://doi.org/10.1002/est2.253

Vance, J. E., & Tasseva, G. (2013). Formation and function of phosphatidylserine and phosphatidylethanolamine in mammalian cells. *Biochimica Et Biophysica Acta-Molecular and Cell Biology of Lipids, 1831*(3), 543–554. https://doi.org/10.1016/j.bbalip.2012.08.016

Verdonschot, P. F. (2015). Introduction to Annelida and the class Polychaeta. In J. H. Thorp & D. C. Rogers (Eds.), *Thorp and Covich's Freshwater Invertebrates: Ecology and General Biology* (pp. 509–528). Academic Press. https://doi.org/10.1016/B978-0-12-385026-3.00020-6

Wijaya, I. D. M. R., Idris, I., Ismail, W. I. W., Asari, A., Harun, N. A., Rudiyanto, R., Tarman, K., Abas, F., & Maulidiani, M. (2024). Discrimination of marine polychaete species of different harvest times using FTIR metabolomics. *Malaysian Journal of Chemistry, 26*(2), 129-138. https://doi.org/10.55373/mjchem.v26i2.129

Yamashita, S., Miyazawa, T., Higuchi, O., Kinoshita, M., & Miyazawa, T. (2023). Marine plasmalogens: A gift from the sea with benefits for age-associated diseases. *Molecules, 28*(17), Article 6328. https://doi.org/10.3390/molecules28176328

Yi, C., Liang, H., Huang, D., Yu, H., Xue, C., Gu, J., Chen, X., Wang, Y., Ren, M., & Zhang, L. (2023). Phenylalanine plays important roles in regulating the capacity of intestinal immunity, antioxidants and apoptosis in largemouth bass (*Micropterus salmoides*). *Animal, 13*(18), 1–14. https://doi.org/10.3390/ani13182980

Zamzam, N. I., Kamarudin, N. I., Idris, I., Harun, N. A., Ismail, W. I. W., & Abas, F. (2021). Investigation of antioxidant activity and chemical fingerprint of marine polychaete based on ATR-FTIR metabolomics. *Universiti Malaysia Terengganu Journal of Undergraduate Research*, *3*(4), 81-88. https://doi.org/10.46754/umtjur.v3i4.241

Zanol, J., da Silva, T., Dos, S. C., & Hutchings, P. (2016). *Marphysa* (Eunicidae, polychaete, Annelida) species of the *Sanguinea* group from Australia, with comments on pseudo-cryptic species. *Invertebrate Biology, 135*, 328–344. https://doi.org/10.1111/ivb.12146

Zeng, M., Tao, J., Xu, S., Bai, X., & Zhang, H. (2023). Marine organisms as a prolific source of bioactive depsipeptides. *Marine Drugs*, *21*(2), Article 120. https://doi.org/10.3390/md21020120

APPENDIX

Investigation of Aged-related Metabolites in the Marine Polychaete *(Marphysa moribidii)* Using [1]H NMR Metabolomics and LC-MS/MS Analysis

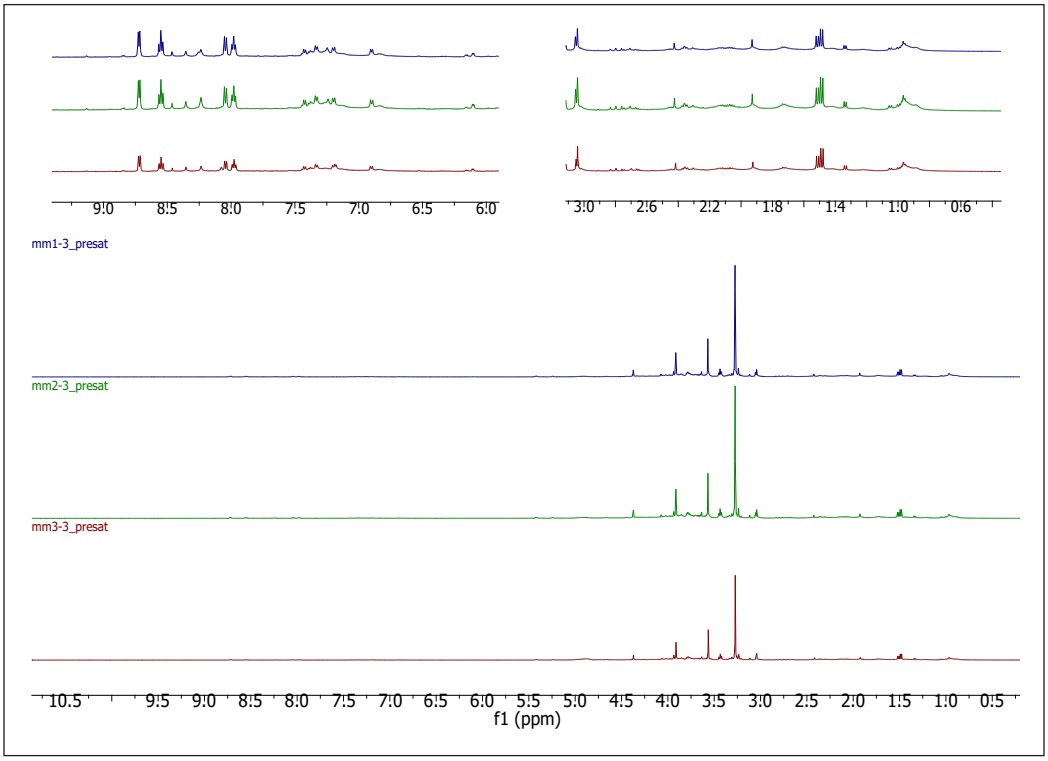

Supplementary Figure 1. Representative [1]H NMR spectra of *M. moribidii* at different ages. Keys: mm1–3 (M1); mm2–3 (M2); and mm3–3 (M3)

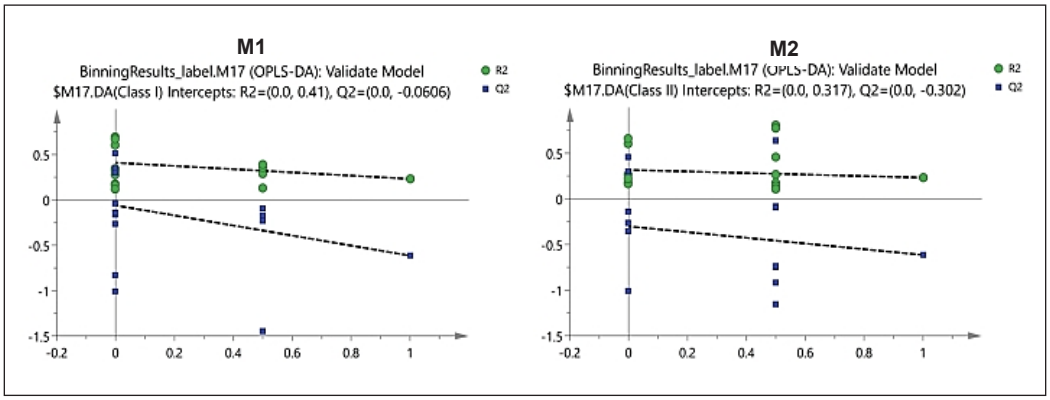

Supplementary Figure 2. Permutation test results of OPLS-DA model M1 versus M2. The permutation tests were carried out with 20 random permutations

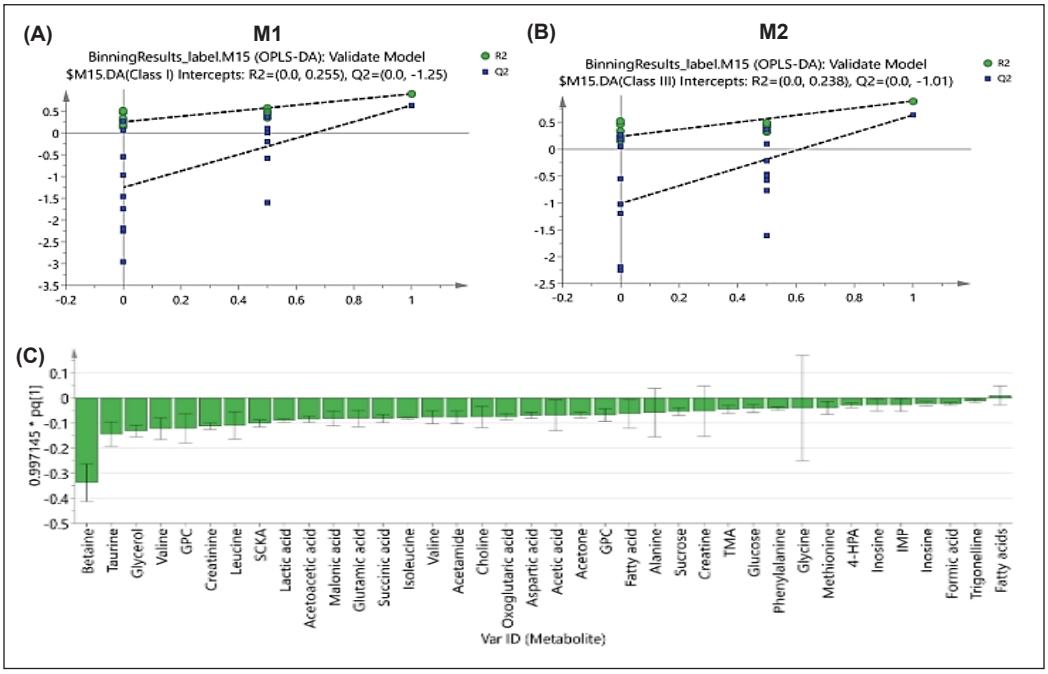

Supplementary Figure 3. OPLS-DA model M1 versus M3 showed the permutation test (20 permutations) results for M1 (A) and M3 (B); and loadings column plot (C)

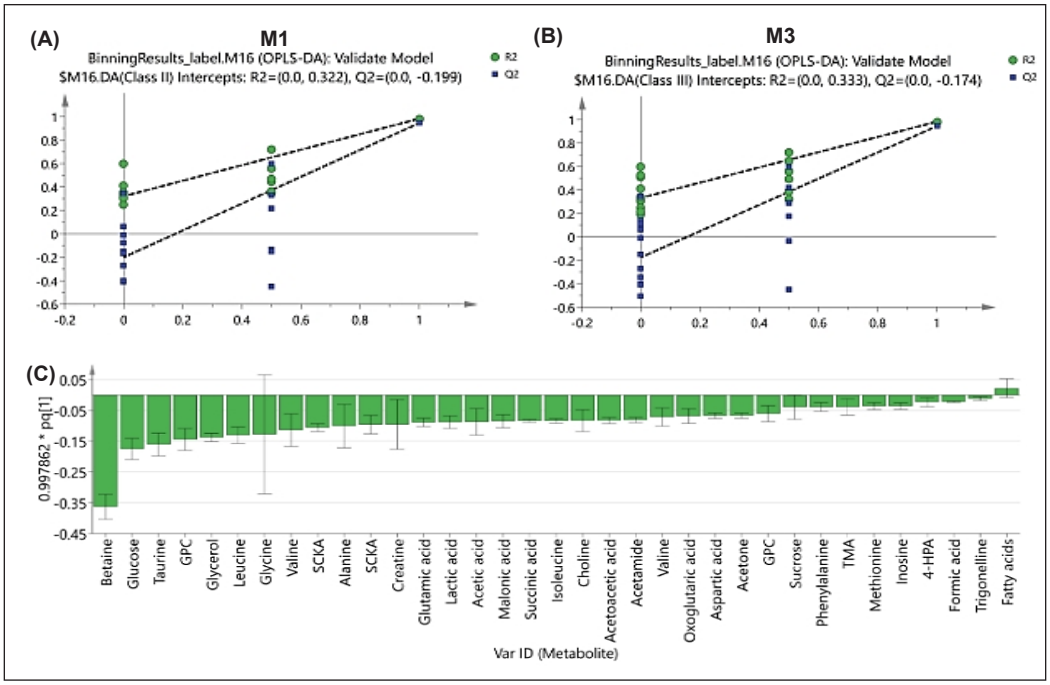

Supplementary Figure 4. OPLS-DA model M2 versus M3 showed the permutation test (20 permutations) results for M2 (A) and M3 (B); and loadings column plot (C)

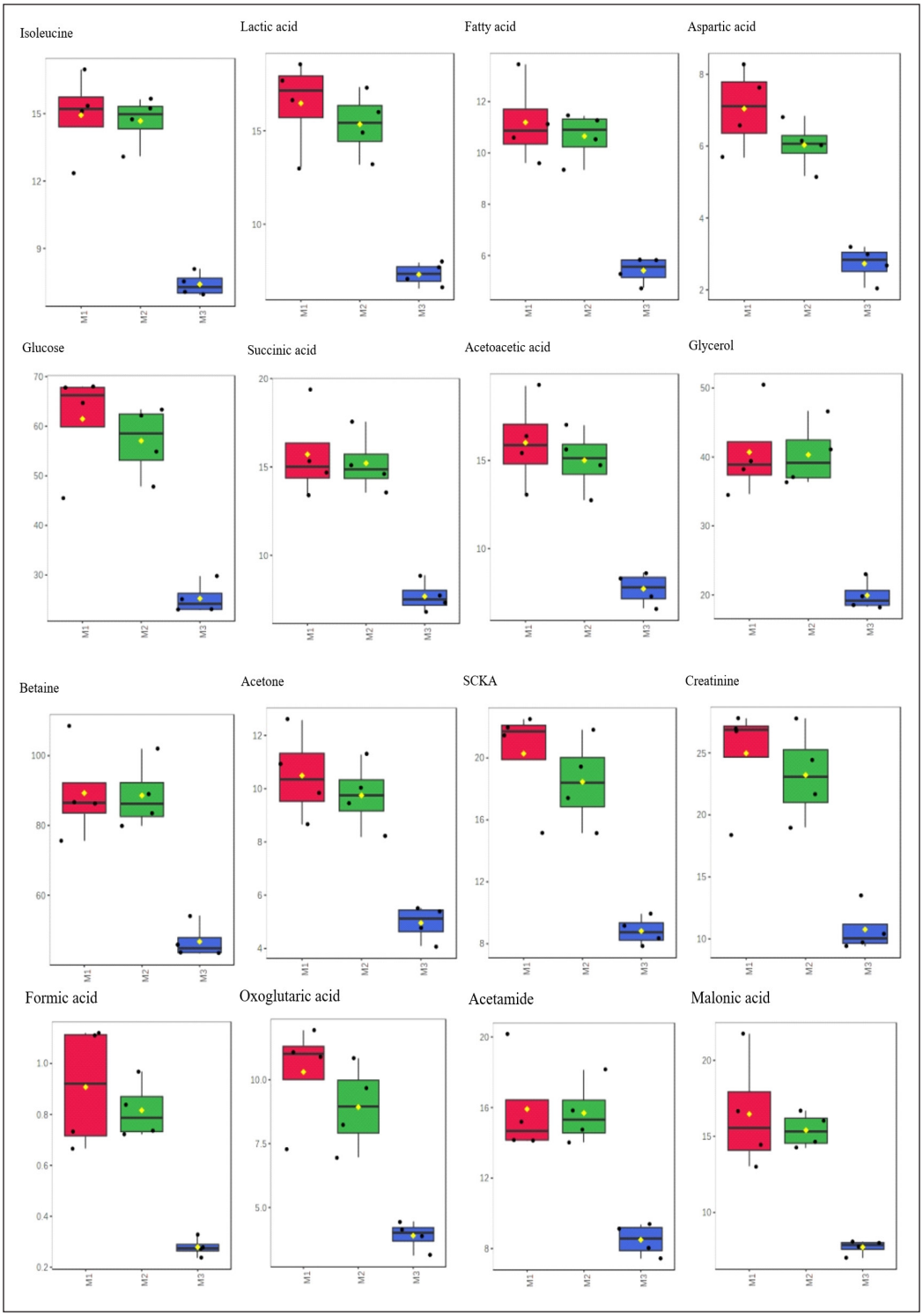

Supplementary Figure 5. Boxplots of M1, M2 and M3 metabolites of the *M. moribidii*

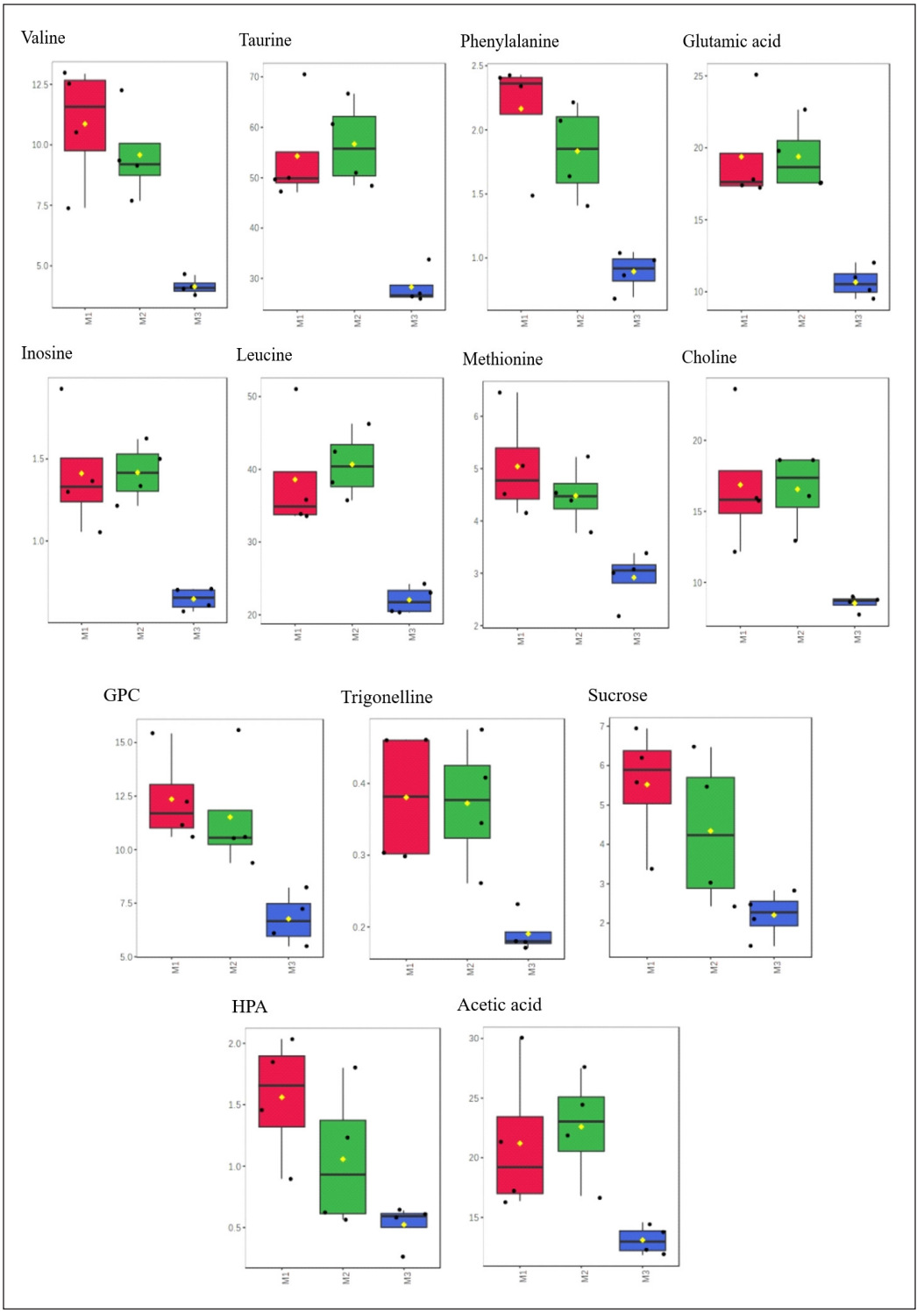

Supplementary Figure 5 (continue). Boxplots of M1, M2 and M3 metabolites of the *M. moribidii*

Supplementary Table 1
One-way ANOVA and Tukey-HSD Pairwise Test results of identified metabolites in M1, M2, and M3

No	Metabolite	δH (ppm)	f.value	p.value	FDR	Tukey's HSD
1	Isoleucine	1.02	42.158	2.69E-05	0.0012837	M3-M1; M3-M2
2	Lactic acid	1.34	31.92	8.19E-05	0.0012837	M3-M1; M3-M2
3	Fatty acid	1.22	31.506	8.62E-05	0.0012837	M3-M1; M3-M2
4	Aspartic acid	2.78	30.054	0.00010381	0.0012837	M3-M1; M3-M2
5	Glucose	3.78	26.308	0.00017396	0.0015077	M3-M1; M3-M2
6	Succinic acid	2.42	23.696	0.00025918	0.0015257	M3-M1; M3-M2
7	Acetoacetic acid	2.30	23.577	0.00026417	0.0015257	M3-M1; M3-M2
8	Glycerol	3.62	23.074	0.00028655	0.0015257	M3-M1; M3-M2
9	Betaine	3.26	22.856	0.00029699	0.0015257	M3-M1; M3-M2
10	Acetone	2.22	22.22	0.00033013	0.0015257	M3-M1; M3-M2
11	SCKA	0.90	21.84	0.00035209	0.0015257	M3-M1; M3-M2
12	Creatinine	3.06	19.301	0.00055558	0.001924	M3-M1; M3-M2
13	Formic acid	8.46	18.968	0.000592	0.001924	M3-M1; M3-M2
14	Oxoglutaric acid	2.46	18.348	0.00066784	0.0020428	M3-M1; M3-M2
15	Acetamide	2.02	17.202	0.00084173	0.0023529	M3-M1; M3-M2
16	Malonic acid	3.10	16.863	0.00090352	0.0023529	M3-M1; M3-M2
17	Creatine	3.02	16.856	0.00090497	0.0023529	M3-M1; M3-M2
18	TMA	2.90	15.07	0.0013405	0.0030708	M3-M1; M3-M2
19	Valine	1.06	15.013	0.0013582	0.0030708	M3-M1; M3-M2
20	Taurine	3.42	14.724	0.0014526	0.0030985	M3-M1; M3-M2
21	Phenylalanine	7.42	14.479	0.0015391	0.0030985	M3-M1; M3-M2
22	Glutamic acid	2.34	14.125	0.0016751	0.003226	M3-M1; M3-M2
23	Inosine	8.34	13.627	0.0018923	0.0034441	M3-M1; M3-M2
24	Leucine	0.94	13.099	0.0021616	0.0037467	M3-M1; M3-M2
25	Methionine	2.62	8.7929	0.0076414	0.012417	M3-M1; M3-M2
26	Choline	3.18	8.6828	0.0079327	0.0125	M3-M1; M3-M2
27	GPC	3.22	7.8935	0.010473	0.015739	M3-M1; M3-M2
28	Trigonelline	8.82	7.8621	0.010594	0.015739	M3-M1; M3-M2
29	Sucrose	5.42	5.2582	0.030711	0.041497	M3-M1
30	4-HPA	6.90	5.2095	0.03141	0.041497	M3-M1
31	Acetic acid	1.90	5.1748	0.031921	0.041497	M3-M2